Journal of Marine Systems 78 (2009) S255–S271

Contents lists available at ScienceDirect

Journal of Marine Systems

journal homepage: www.elsevier.com/locate/jmarsys

An evaluation of a high-resolution operational wave forecasting system in the Adriatic Sea

J.D. Dykes *, D.W. Wang, J.W. Book

Oceanography Division, Naval Research Laboratory, 1009 Balch Blvd, Stennis Space Center, Mississippi, 39529, USA

ARTICLE INFO

Article history:
Received 31 March 2008
Received in revised form 16 December 2008
Accepted 22 January 2009
Available online 1 March 2009

Keywords:
Adriatic Sea
Atmospheric forcing
Model validation
Operational forecasting
Wave forecasting
Wave modeling

ABSTRACT

The SWAN (Simulating Waves Nearshore) wave model using wind inputs generated by the ALADIN 8-km, operational high-resolution, atmospheric model was run in real-time to provide surface waves forecast for the semi-enclosed Adriatic Sea in support of the "Dynamics of the Adriatic in Real-Time" (DART) field experiments. Together with predictions from other wave and wind models, the successful prediction of a high sea-state event by this model led to a real-time shifting of planned operations while at sea, allowing five ADCP moorings to be deployed just before a bora storm and associated storm waves arrived. The model was also able to simulate the spatial gradients in significant wave height observed by in-situ and remote-sensing measurements for a particular sirocco storm case study, providing an additional perspective in aiding interpretation of the model output of features. To further quantify prediction skill, the wave forecast performance over a 12-month period was evaluated against in-situ and altimeter measurements over the region. Correlation coefficients between forecast and in-situ measured significant wave heights were from 0.82 to 0.91 for the 24-h forecast and from 0.78 to 0.88 for the 48-h forecast. However, best-fit slope comparisons with in-situ wave data at five coastal locations show the forecast wave heights were underpredicted by 10% to 30%. Best-fit slope comparisons between modeled wind speeds, U_{10}, and significant wave heights, H_s, and altimeter-derived measurements show that model U_{10} was about 4% underpredicted, but H_s was underpredicted by an average of 30%. The underprediction of SWAN H_s has a very significant location-dependent geographical variation ranging from 10% to over 50%. In addition, the wave model comparison with altimeter H_s shows a broad region of scatter index exceeding 0.4 along and offshore of the central Croatian coast. Elsewhere the scatter index is generally around 0.3. Compared to previous studies we found that using higher-resolution wind forcing with realistic orography decreased the U_{10} underestimation bias, but the magnitude of H_s underestimation bias did not correspondingly decrease, suggesting that wave model dynamics or wind–wave coupling deserves further investigation.

Published by Elsevier B.V.

1. Introduction

Operational requirements for nowcast/forecast wave models include the ability to predict the spatial locations and arrival times of sharp significant wave height (H_s) gradients and thus be able to assure the planning of safe ship operations before or after the arrival of high seas or at locations with low H_s during times when there are strong spatial H_s gradients. It was partially for such operational reasons that the Naval Research Laboratory (NRL) ran a forecast SWAN (Simulating Waves Nearshore) wave model in real-time for the Adriatic Sea in 2006. At the time, NRL was participating in an internationally collaborative project, "Dynamics of the Adriatic in Real-Time" (DART), jointly with the NATO Undersea Research Centre (NURC) and many other partners. One of the main goals of the effort was to evaluate monitoring and prediction capabilities for vigorous, swiftly-evolving fronts and eddies in a topographically controlled coastal environment. To accomplish this, mooring measurements; drifter data; towed Conductivity–Temperature–Depth (CTD) measurements; turbulence profile measurements; numerous standard CTD profiles; surface wave measurements; remote sensing of temperature, optics, and roughness; high-resolution atmospheric models; high-resolution ocean models; and wave models were all utilized (see various other manuscripts in this special issue). A key part of the logistics of the project was the deployments and recoveries of 16 different bottom moorings, at various times over the 12-month period, October 2005 through September 2006. Due to limits on deployment time from corrosion or battery life, all of these moorings were deployed and recovered twice, typically with a deployment in October, recovery and redeployment in March, and a final recovery in September. With such a large number of deployments and recoveries (especially in March 2006) and limited ship time for these and other DART objectives, the wave model forecasts were very useful in efficiently planning the timing and order of mooring operations and avoiding sea-state conditions that were too severe to permit mooring work.

* Corresponding author. Tel.: +1 228 688 5787; fax: +1 228 688 4759.
E-mail address: james.dykes@nrlssc.navy.mil (J.D. Dykes).

0924-7963/$ – see front matter. Published by Elsevier B.V.
doi:10.1016/j.jmarsys.2009.01.027

In addition to practical needs, the DART international project was also generally focused on evaluating rapid environmental assessment (REA) capability using multiple models. Therefore, NURC encouraged various partners to run operational models of various processes, including waves, during the two focused REA experiments in March and September 2006. Thus, in total, four different state-of-the-art operational wave forecast models were run and used during the experiments. These were: (1) a 1/12 degree or 8-km SWAN model forced by LAMI (Limited Area Model Italy) (Signell et al., 2005), a 7-km Italian operational model for medium- and small-scale weather prediction based on a model developed by the German Meteorological Service (Deutscher Wetterdienst) (Steppler et al., 2003); (2) a 1/20-degree or 5-km WAve Model Cycle 4 (WAM, (WAMDI group, 1988; Komen et al., 1994)) forced by SKIRON, a 1/20-degree modified version of the Eta/NCEP model (Kallos et al., 1997, 2006); (3) a 1/12-degree or 8-km WAM forced by the ECMWF (European Centre for Medium Range Weather Forecasting) model (Janssen et al., 1997); and (4) a 5-km SWAN model forced by 8-km ALADIN wind model (see Sections 2 and 3 for details). Model (1) was run by Servizio Idro-Meteo-Clima ARPA-SIMC of Emilia Romagna Region, Bologna, Italy; model (2) was run by the University of Athens; model (3) was run by the Marine Science Institute of the Italian National Research Council; and model (4) was run by NRL as first mentioned above.

During the March experiment, all available wave model forecast data were transferred to R/V Alliance while at sea, and displayed together with the same graphics and scales to provide a simple planning tool for the chief scientist to potentially change daily activities. Through this process it became immediately clear that all four models were often displaying quite different spatial H_s patterns for the same wind events. Fig. 1 shows one example of this; the 48-h H_s forecasts greatly differ between SWAN-LAMI (model 1), WAM-SKIRON (model 2), and SWAN-ALADIN (model 4). In other instances the patterns disagree in different ways but to the same extent with, e.g., in a different snapshot (not shown) SWAN-LAMI (model 1) and SWAN-ALADIN (model 4) were similar to each other but different than the other two models. Given the complexity of the Adriatic orography and winds (Pasarić et al., 2009-this issue), this is perhaps not surprising, but it also suggests that there is a need for validating spatial accuracy for operational wave modeling in such coastal environments so that confidence can be placed in more complex predicted spatial patterns of H_s and operations can be optimized with respect to wave conditions. For example, in this forecast snapshot (Fig. 1), the predicted H_s values with respect to the southern DART moorings (solid circles) are not consistent and therefore it would be unclear if the sea-state conditions would have allowed for recovery or deployment operations at that time.

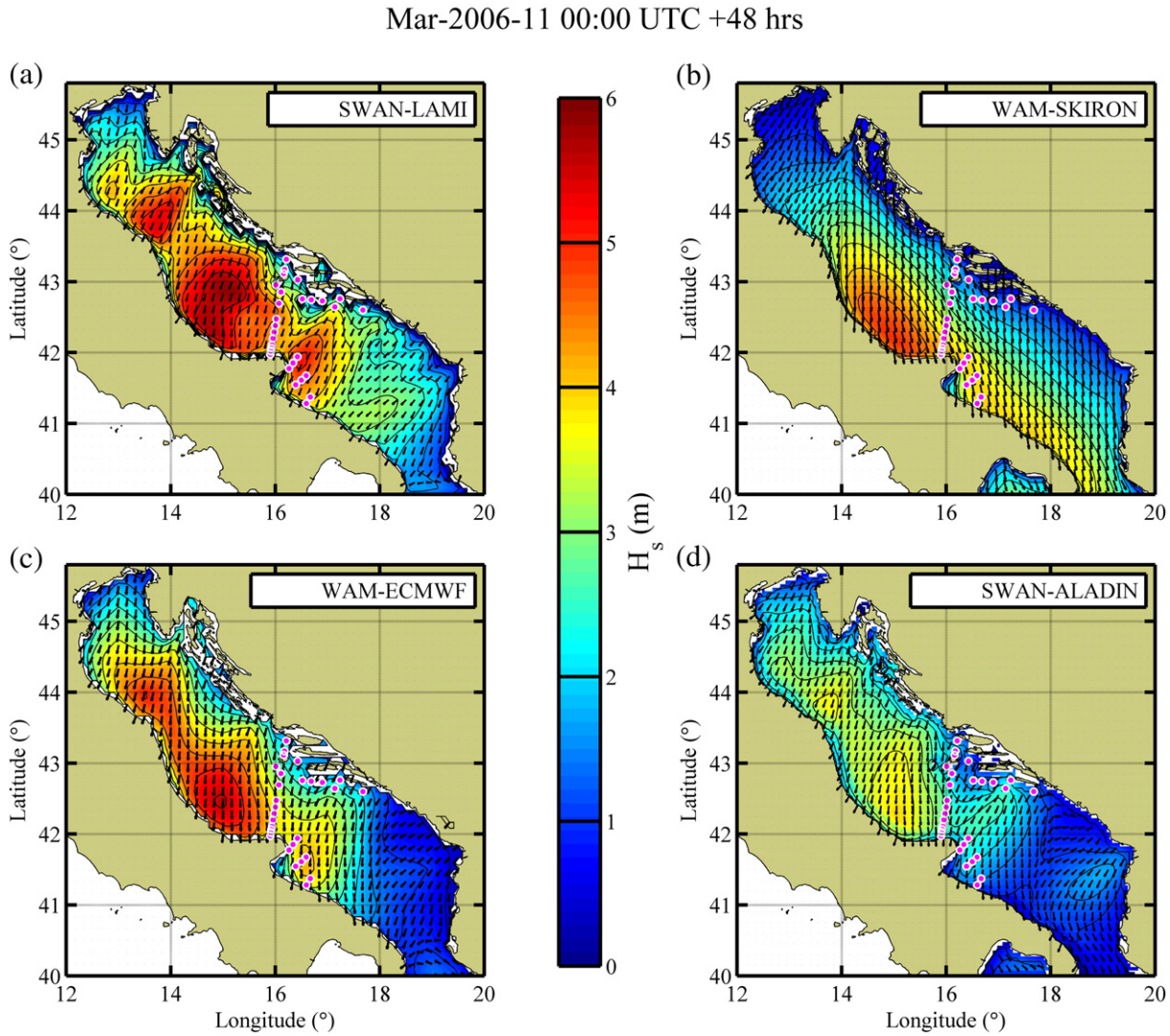

Fig. 1. 48-h forecast wave field valid for 00 UTC, March 13, 2006 by the four models forced by their associated wind models indicated in the hyphenated names: (a) SWAN by LAMI, (b) WAM by SKIRON, (c) WAM by ECMWF, and (d) SWAN by ALADIN. DART observation network is shown as solid circles.

Thus, in this paper we conducted a spatially oriented evaluation of the NRL SWAN model as a case study of wave forecast model validation in such situations. Through their multi-model ensemble work, Lenartz et al. (2007) compared all four operationally wave models shown in Fig. 1 against a limited set of observational metrics in the central Adriatic and has shown that the NRL SWAN model is not anomalous in accuracy with respect to the others. Therefore, the techniques applied here should be generally applicable to operational wave models of the Adriatic and also likely elsewhere in similarly complex regions. Furthermore, Fig. 1 directly demonstrates the importance of understanding spatial accuracy with regard to full utilization of wave model forecasting for operational efforts in coastal seas.

The Adriatic Sea (Fig. 2) is a semi-enclosed basin about 750 km long and 250 km wide with a connection to the Mediterranean Sea at the Strait of Otranto (72 km wide, 780 m deep). As others have done before us (e.g. Janeković and Tudor, 2005) we take advantage of the fact that this basin is practically isolated and neglect incoming wave energy from the Mediterranean Sea, keeping in mind that in some situations and in particular locations near Otranto neglecting such waves might lead to greater errors in the model. The mountain ridges surrounding the Adriatic Sea induce a strong topographic effect into the wind field. Strong winds and large waves are often generated by two dominant wind regimes affecting the Adriatic Sea (Cushman-Roisin et al., 2001). During winter, the dominating wind called the bora (a.k.a. "bura") is a northeasterly wind that crosses the northern Adriatic and is influenced by catabatic flow. Mainly during spring and autumn the main wind of concern is a southeasterly wind called the sirocco (a.k.a. scirocco or jugo), which flows along the main axis of the basin. The relative small and semi-enclosed regular basin and strong wind events from along-basin (sirocco) and cross-basin (bora) directions thus make the Adriatic Sea an ideal but challenging place to examine and evaluate wind–wave modeling capability (Cavaleri et al., 1989).

Many institutions run global and regional atmospheric and wave models producing daily forecasts that provide coverage over the Adriatic Sea (Signell et al., 2005; Cavaleri and Sclavo, 2006). A few evaluation studies focused on wave prediction in the Adriatic Sea. (Cavaleri et al., 1989; Bertotti et al., 1996; Cavaleri et al., 1996; Cavaleri and Bertotti, 1997; Signell et al., 2005; Janeković and Tudor, 2005). Often, due to its complexity near the coast and its fundamental importance to waves, studies have focused on the role of wind accuracy with regard to wave accuracy in the Adriatic and similar regions. Cavaleri and Bertotti (2004) showed that waves in areas of semi-enclosed and enclosed basins could be underestimated due to lower wind forcing produced by a coarser resolution atmospheric model that inadequately addresses effects of complex orography of the region. One commonly used approach to partially compensate for this problem is to apply an enhancement factor to the wind field with the value decreasing as the resolution of the wind model increases (Cavaleri and Bertotti, 1997; Cavaleri, 2002). Signell et al. (2005) showed that using non-hydrostatic meteorological models in the Adriatic Sea with increased spatial resolution of 7 km or 4 km could improve the overall performance of SWAN simulations at three coastal stations for a 2-month period as compared to runs conducted with 40-km or 20-km resolution hydrostatic wind models.

In this study, we ran high-resolution SWAN using input winds from an 8-km operational high-resolution ALADIN model in the Adriatic Sea during the period starting in September 2005 through October 2006. The evaluation is based on comparisons between models and in-situ and satellite-borne altimeter measurements in order to maximize spatial coverage over the Adriatic. Others have examined the spatial distribution of wave model accuracy using buoys and altimeters before

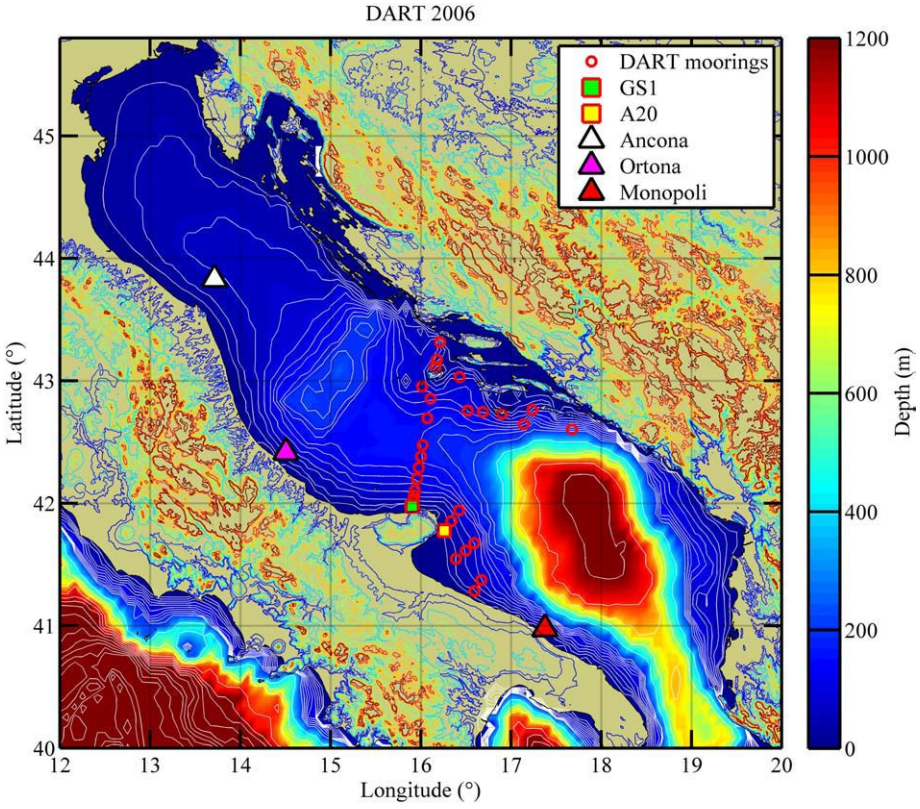

Fig. 2. Bathymetry map of the Adriatic Sea and in-situ observation network layout during DART experiment (red circles). The in-situ wave data from two DART mooring sites in nearshore waters around Cape Gargano, GS1 (solid green square) and A20 (solid yellow square), and three RON buoys at Ancona (solid white triangle), Ortona (solid pink triangle) and Monopoli (solid red triangle) were used for validating NRL SWAN wave simulations.

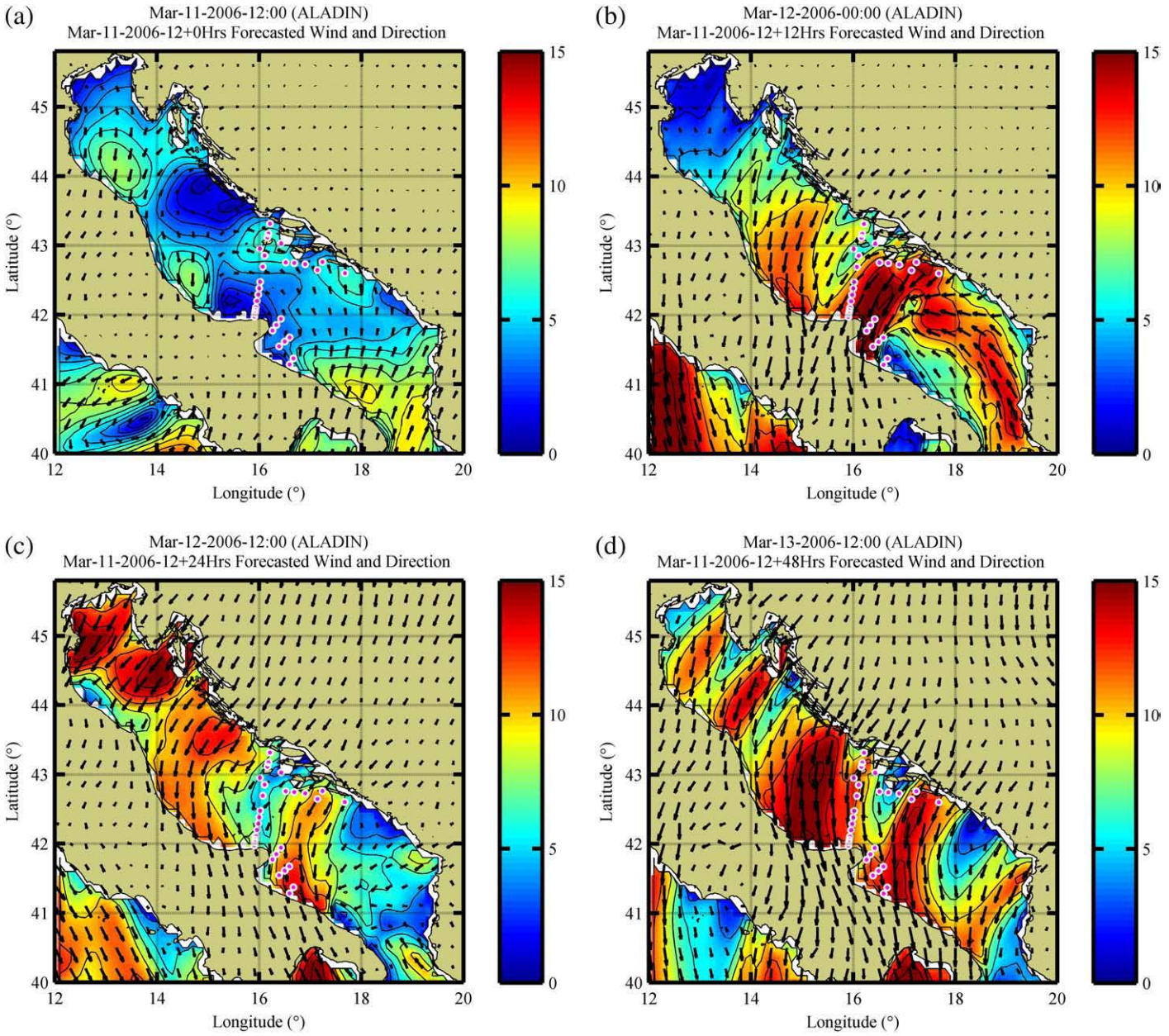

Fig. 3. Snapshots of a forecast wind field evolution over the Adriatic Sea by the ALADIN model run at 12 UTC, March 11, 2006; (a) 0-h nowcast (b) 12-h forecast at 0 UTC, March 12, (c) 24-h forecast at 12 UTC, March 12, and (d) 48-h forecast at 12 UTC, March 13. Color bars shown indicate wind speed, U_{10}, in m/s and arrows indicate wind speed and direction. The arrow length is scaled by wind speed. DART observation network is shown as solid circles.

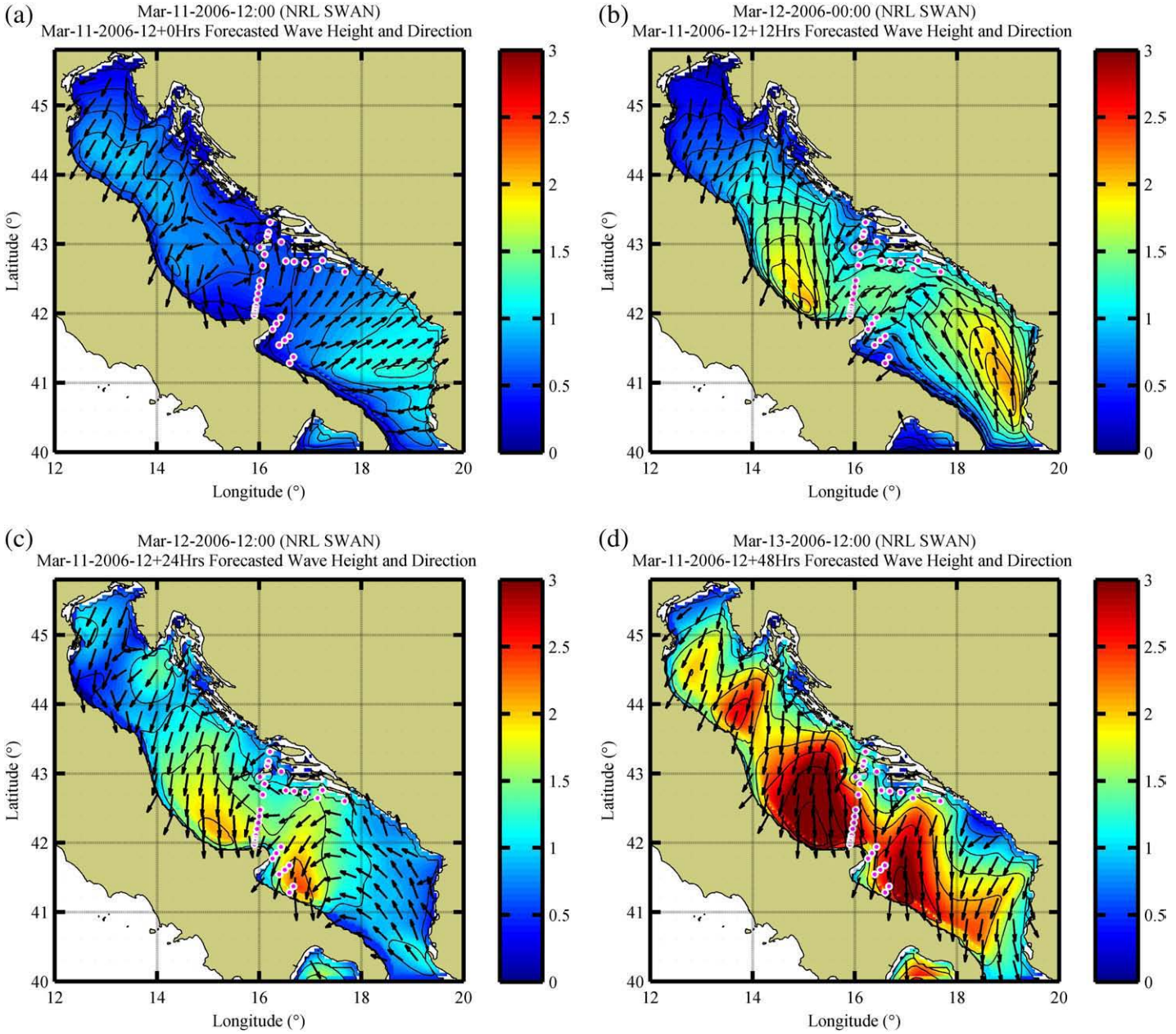

Fig. 4. Snapshot of a forecast wave field evolution over the Adriatic Sea by the NRL SWAN run at 12 UTC, March 11, 2006; (a) 0-h nowcast (b) 12-h forecast at 0 UTC, March 12, (c) 24-h forecast at 12 UTC, March 12, and (d) 48-h forecast at 12 UTC, March 13. Color bars shown indicate significant wave height, H_s, in m and arrows indicate prevailing wave direction. DART observation network is shown as solid circles.

(e.g., Cavaleri and Sclavo, 2006), but not with a wave model forced by a wind model that adequately resolves much of the complex orography and produces realistic small-scale, spatial structure. Therefore, in this paper we undertake such an analysis, building upon the Signell et al. (2005) evaluation of wave model accuracy at three locations for a similarly driven wave model.

2. ALADIN meteorological model

It is clear that the accuracy of wave models is highly dependent on the accuracy of meteorological models that force them and thus must be studied closely with this in mind. For smaller scales less than synoptic and in regions with interesting orographic features, accurate atmospheric modeling is particularly challenging. There have been many studies on the effects of wind fields on wave models used in enclosed, semi-enclosed, or relatively small basins (Signell et al., 2005; Ardhuin et al., 2007; Bolanos-Sanchez et al., 2007). The general consensus is that higher-resolution models are essential in smaller seas where locally generated waves are primary. In this study, an 8-km resolution wind forecast was obtained by using the Croatian version of the operational meso-scale meteorological model, ALADIN, which is a limited-area model (LAM) built on the basis of the global model IFS/ARPEGE (ARPEGE — Action de Recherche Petite Echelle Grande Echelle, IFS — Integrated Forecast System). The ALADIN runs operationally for 00 and 12 UTC at the Croatian Meteorological and Hydrological Service and provides 48-h wind forecasts (Ivatek-Šahdan and Tudor, 2004; Pasarić et al., 2007). The model forecasts were first obtained using ALADIN on a LACE domain that covers most of Europe with 12-km resolution. The initial and boundary conditions were obtained from the analysis and forecasts of the global model ARPEGE run in Meteo-France, with DFI (digital filter initialization) on the analysis. The European domain output fields are dynamically adapted to the Croatian domain with 8-km resolution using the 48-h integration of the ALADIN model and the full physics package. This provided a finer spatial resolution and more realistic depiction of the land-sea mask and orography by the ALADIN model and facilitated output of improved meteorological products for operations and research (e.g., see Pasarić et al., 2007). More details about the developments and validations of ALADIN/Croatia can be found in Ivatek-Šahdan and Tudor (2004).

3. SWAN wave model

SWAN is a third-generation wave model originally developed for shallow water at Delft University of Technology (TU Delft) in the Netherlands (Holthuijsen et al., 1989; Booij et al., 1999; Ris et al., 1999; and http://www.swan.ct.tudelft.nl). The earlier version of SWAN was not recommended to be run at scales larger than 25 km due to diffusion problems. This problem has been discussed and resolved by Rogers et al. (2002). SWAN was then recommended to be used on any scale relevant for wind generated surface gravity waves (SWAN user manual cycle III version 40.51). SWAN then has been used to study wave conditions in larger areas such as semi-enclosed basins (Signell et al., 2005) and enclosed lakes (Rogers et al., 2003). The balance

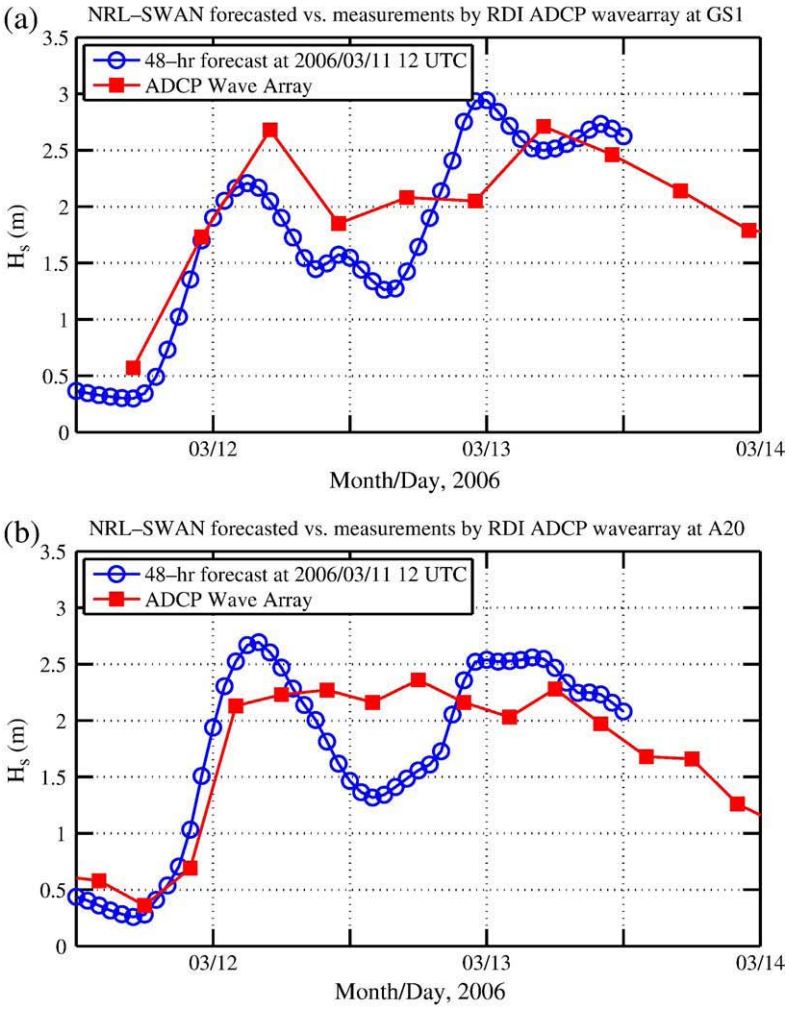

Fig. 5. Time history of significant wave height, H_s, from in-situ measurements and 48-h SWAN wave forecast run at 12 UTC, March 11, 2006 at two mooring sites: (a) GS1 and (b) A20.

equation of the two-dimensional wave action density spectrum includes local rate of change in time, propagation, and depth-induced and current-induced refraction and shoaling. The sink and source terms include wind generation, white-capping dissipation, depth-induced wave breaking, bottom friction, and non-linear wave–wave interactions. Thus, the primary input is a wind field at or near the surface usually from an atmospheric model which produces daily forecasts. Another important input is the bathymetry which is normally static. The bathymetry used in this study was derived from a database developed by the Naval Oceanographic Office and nautical chart soundings (Fig. 2). The domain used for DART is a grid with 181 columns and 141 rows on a spherical coordinate system with a uniform resolution of 1/20° longitude and latitude (about 5 km). Although the grid extends beyond the southern and south-western shores of Italy, those points were ignored. SWAN linearly interpolated the bathymetry and the wind components from the ALADIN meteorological model on to the SWAN computational grid. The model in this study was run in non-stationary mode with depth-induced wave breaking turned off since no surf zones are considered here, but default bottom friction parameters were left on to consider the effects of shoaling and refracting in shallow water. With a model time step of 20 min, each run took about 15 min of wall-clock time using four processors making it practical to run the model every 12 h in real-time to support DART operations providing predictions up to 48 h of significant wave height, peak wave direction and peak wave period. This operational effort follows extensive previous work at improving operational modeling systems for rapid environmental assessment (Allard et al., 2002, 2007; Dykes et al., 2004; Hsu et al., 2002; Jensen et al., 2002; Rogers et al., 2007). In addition, for the purposes of comparing with a larger set of observations from altimeters and in-situ moorings, SWAN was rerun simulating operations from mid-September 2005 through October 2006 by producing 48-h forecasts every 12 h.

4. Evaluation of model performance

The surface waves in a small and semi-enclosed basin can grow very rapidly both in space and time. To illustrate this point, snapshots of wind and wave fields at selected forecast hours from a 48-h ALADIN and SWAN forecast runs at 12 UTC, March 11, 2006 are shown in Figs. 3 and 4, respectively. The wind field is represented by wind speed at 10 m above the surface (U_{10}) and the significant wave height field is represented by H_s. The wind condition over the entire Adriatic Sea was relatively calm with U_{10} mostly less than 5 m/s (Fig. 3a) at the beginning of the 48-h period. However, within 12 h, a strong northerly wind with speeds higher than 15 m/s was present in the DART mooring network area (Fig. 3b). Strong bora winds covered most of the region in the next two days (Fig. 3c and d). As a result, H_s in the Italian coastal waters increased from less than 0.5 m to 3 m (Fig. 4a and d) during this 48-h period. There were distinct spatial gradients in H_s and a few regions were forecast to remain relatively calm even during the peak of the storm. The validity of such wave forecasts will be studied against in-situ and altimeter measured H_s in the next three sub-sections.

4.1. Comparison with in-situ measurements

The in-situ wave data used in this study are from two NRL DART mooring stations and three coastal buoys of the Italian National buoy network RON (Rete Ondametrica Nazionale). The in-situ DART wave data came from the two shallowest deployed ADCPs (Acoustic Doppler Current Profiler) along the 17-m isobath at DART mooring sites of GS1 (Oct. 2005 to Sep. 2006) and A20 (Oct. 2005 to Mar. 2006 and Aug. 2006 to Sep. 2006). At the sea floor of each site, we deployed an upward-looking 1200 kHz Teledyne/RD Instruments Workhorse Sentinel equipped with special wave tracking hardware and software. These ADCPs combined measurements of orbital velocities of waves, acoustic

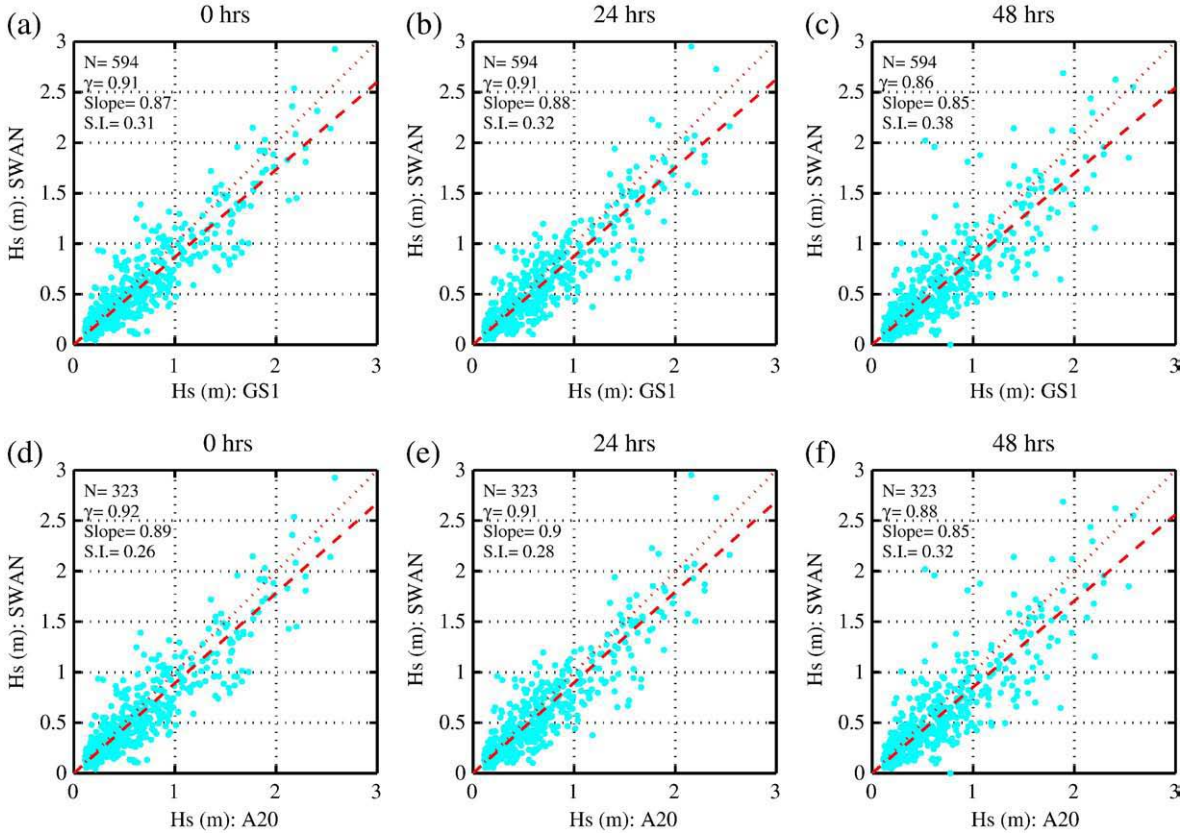

Fig. 6. Comparison of in-situ measured H_s versus 48-h SWAN forecast H_s at GS1: (a) nowcast, (b) 24-h and (d) 48-h forecast; at A20: (d) nowcast, (e) 24-h and (f) 48-h forecast. Dotted line represents 1:1 ratio and dashed line represents the slope of best-fit line.

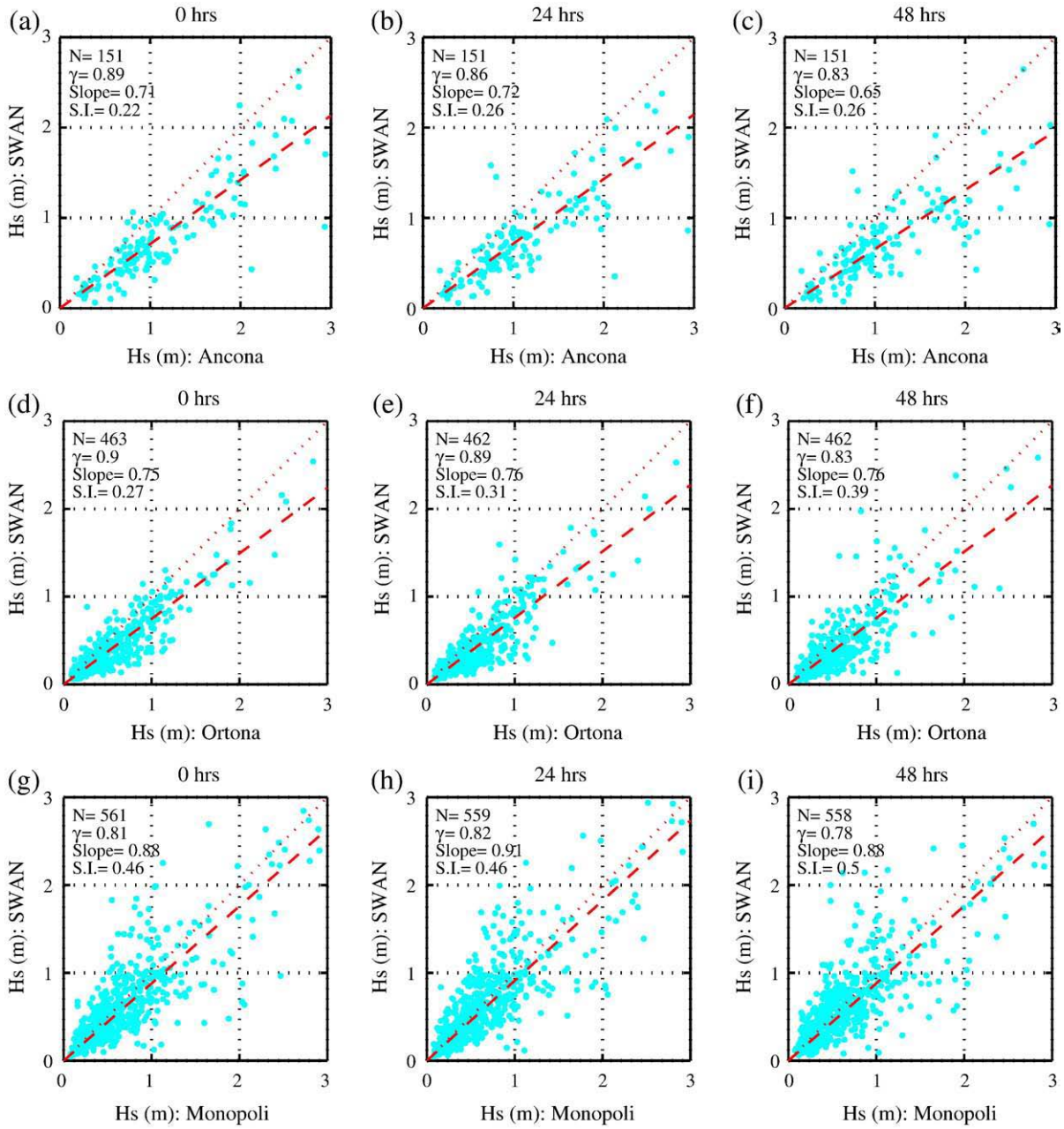

Fig. 7. Scatter plots of 48-h SWAN forecast H_s versus in-situ RON buoy H_s at Ancona (a) nowcast, (b) 24-h and (c) 48-h forecasts; RON buoy at Ortona (d) nowcast, (e) 24-h and (f) 48-h forecasts and RON buoy at Monopoli (g) nowcast, (h) 24-h and (i) 48-h forecasts. The dotted line represents 1:1 ratio and dashed line represents the slope of best-fit line.

tracking of the sea surface, and pressure fluctuations to produce estimates of surface gravity wave parameters and spectra (Strong et al., 2000, RD Instruments, 2001). GS1 and A20 were set up to measure waves every 4 h using 1200 pings taken at 2 Hz (i.e., 10-min duration wave bursts) from October 2005 through March 2006. The settings were changed on GS1 in March to extend battery life, reducing the wave measurement interval to every 6 h and using only 1080 pings (9-min duration wave bursts). A20 in August and September 2006 measured waves every 2 h, and reverted back to using 1200-ping bursts.

Fig. 5 shows the time history of measured H_s at GS1 and A20 during the bora event depicted in Fig. 4. Also shown are results from a 48-h wave forecast by the NRL SWAN run at 12 UTC, March 11, 2006. Model H_s values were spatially interpolated from the model grid to the locations of GS1 and A20. The wave conditions at these two mooring sites were forecast to have a rapid increase from less than 0.5 m to exceed 2 m at the end of March 11, 2006. The wave conditions at the two sites were forecast to increase again in later hours of March 12. The comparisons against measured waves show that the first high wave event was well forecast regarding the arriving time. The magnitudes of H_s were slightly

Table 1
Summary of statistics of comparison between forecast SWAN and in-situ measured significant wave height (H_s) at two DART moorings and three RON buoys.

Stations	Best-fit Slope			Scatter Index (SI)			Correlation Coefficient		
	0 h	24 h	48 h	0 h	24 h	48 h	0 h	24 h	48 h
GS1 (DART)	0.87	0.88	0.85	0.31	0.32	0.38	0.91	0.91	0.86
A20 (DART)	0.89	0.9	0.85	0.26	0.28	0.32	0.92	0.91	0.88
Ancona (RON)	0.71	0.72	0.65	0.22	0.26	0.26	0.89	0.86	0.83
Ortona (RON)	0.75	0.76	0.76	0.27	0.31	0.39	0.90	0.89	0.83
Monopoli (RON)	0.88	0.91	0.88	0.46	0.46	0.5	0.81	0.82	0.78

Scatter index is defined as the root-mean-square difference from the best-fit line divided by the mean measured values.

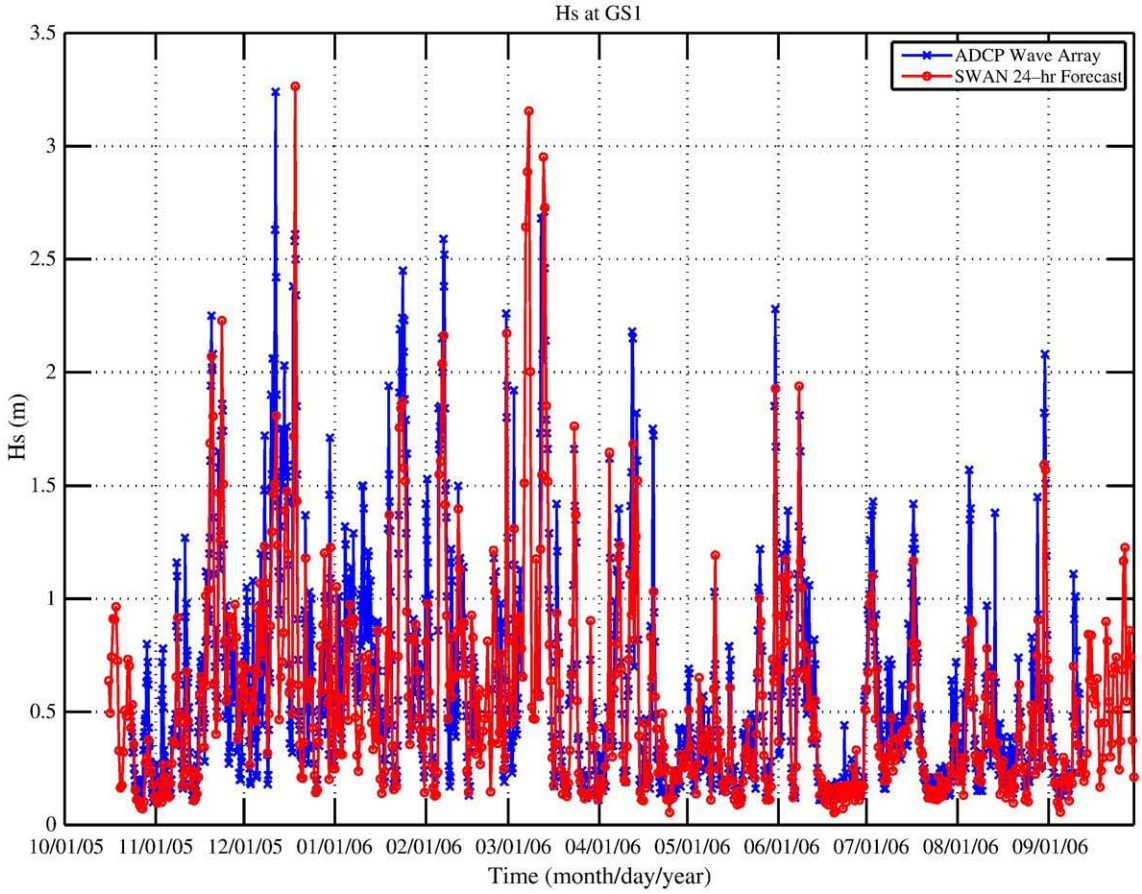

Fig. 8. Time history of in-situ measured H_s and SWAN 24-h forecast H_s at GS1.

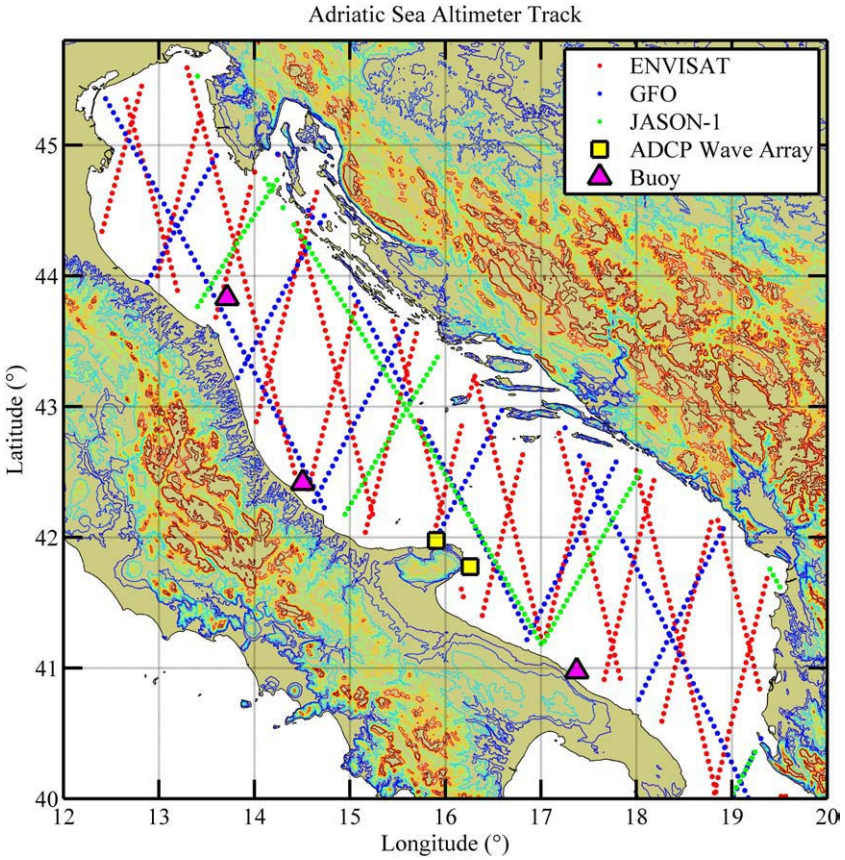

Fig. 9. ENVISAT, GFO, and JASON-1 satellite tracks over the Adriatic Sea. In-situ wave measurement sites are indicated by two solid yellow squares for DART moorings and three solid pink triangles for RON buoys.

underpredicted at GS1 and overpredicted at A20. The accuracy of the wave forecast decreased in later hours of the 48-h forecast period. As a result, the forecast H_s variations after 12 UTC, March 12 did not agree well with ADCP wave measurements. However, the differences are still within sea-state thresholds of many operational activities. During the operation of DART, the real-time wind and wave forecasts of this storm

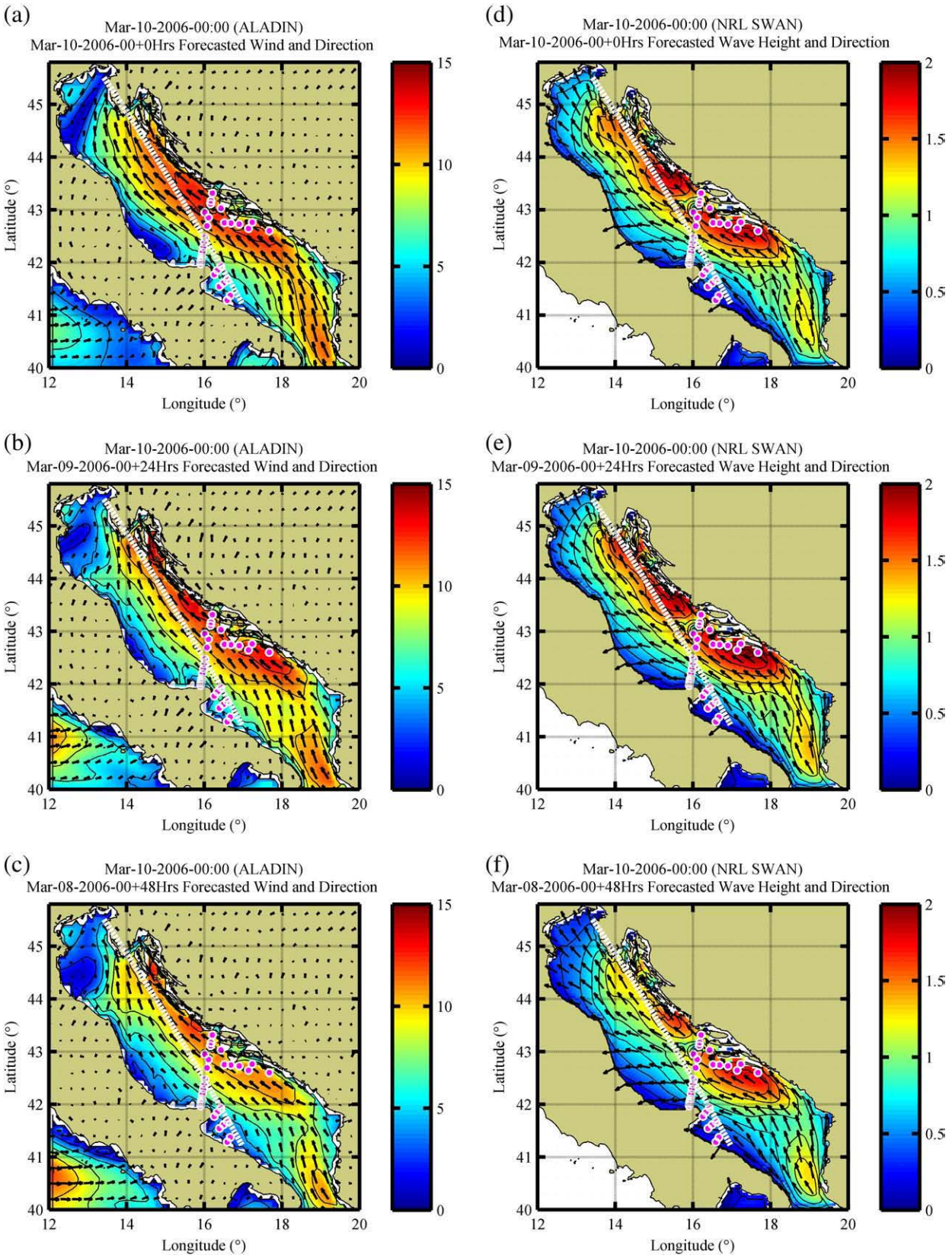

Fig. 10. Wind field at 0 UTC, March 10, 2006 by ALADIN of (a) nowcast, (b) 24-h and (c) 48-h forecasts. Wave field at 0 UTC, March 10, 2006 by SWAN of (d) nowcast, (e) 24-h and (f) 48-h forecasts. White dashed lines represent the JASON-1 satellite track during the time period from 00:21 UTC to 00:23 UTC March 10, 2006. Color bar indicates wind speed in m/s and significant wave height in meters. DART observation network is shown as solid circles.

event compiled from all the various models motivated a change in ship activity for March 11, and mooring redeployment (high sensitivity to sea-state) was moved ahead of a multi-day Aquashuttle CTD Tow-Yo survey (less sensitive to sea-state). Thus, 5 ADCP moorings were redeployed (including GS1) on March 11 just before the forecast storm and storm waves arrived (note in Fig. 5 that only the first wave measurement that was redeployed after GS1 showed relatively calm seas).

To further quantify the difference between SWAN forecast H_s and in-situ measurements, measured H_s was temporally interpolated to the SWAN forecast hours. The scatter plots of interpolated in-situ H_s and SWAN forecast H_s of 0-h (nowcast), 24-h and 48-h are shown in Fig. 6. Forecast H_s at GS1 correlate well with measured data with correlation coefficients larger than 0.9 (Fig. 6a and b). There is only a slight decrease in correlation to 0.86 for the 48-h forecast. The slope of the best-fit line between measured and model data provides an estimate of the local average ratio (Cavaleri and Bertotti, 2006). A slope with a value less than unity indicates an underprediction ratio by the model. The best-fit slope at GS1 is 0.87 for the 0-h nowcast and drops to 0.85 for the 48-h forecast. Similar results are also shown at A20. In general, model H_s was underestimated by about 10 to 15% at these two locations.

We also examine wave model performance outside the DART experiment area by comparing forecast H_s against wave data from three coastal buoys (Ancona, Ortona, and Monopoli) of the Italian National buoy network RON (Rete Ondametrica Nazionale) operated by APAT (Agenzia per la Protezione dell'Ambiente e per i Servizi Tecnici). More details about this network and operation can be found in Arena et al. (2001) and Piscopia et al. (2002). The scatter plots of forecast H_s against buoy waves at these three buoys are shown in Fig. 7. Comparisons show that model H_s at these buoys was underestimated with the best-fit slopes of 0.71, 0.75, and 0.88. I.e., the underprediction was much larger at Ancona and Ortona buoys. The statistics of the comparison for the NRL SWAN wave model nowcast, 24-h and 48-h forecasts at the five locations are summarized and displayed in Table 1.

Compared to the same wave buoys, albeit for a different time period, NRL SWAN had slightly higher correlation coefficients (Table 1) than any of the four models used by Signell et al. (2005), indicating the degree of skill of NRL SWAN in matching the timing and fluctuations of wave events. This can be further seen in Fig. 8, which shows the NRL SWAN 24-h forecast for the entire year at site GS1 and the measured H_s by the moored ADCP. NRL SWAN predicted the occurrence of most of the major wave events (correlation coefficient 0.91) even if often underpredicting the peak H_s value. Such performance is probably sufficient in most cases for an operational user to avoid planning activities at site GS1 during times of high sea-state. However, depending on the particular H_s threshold of the planned activity, there would be times when the model would have been deficient in this regard, most notably for the strong wave event in mid-December with a measured H_s peak over 3 m but a forecast of only a broad increase in H_s to values less than 2 m.

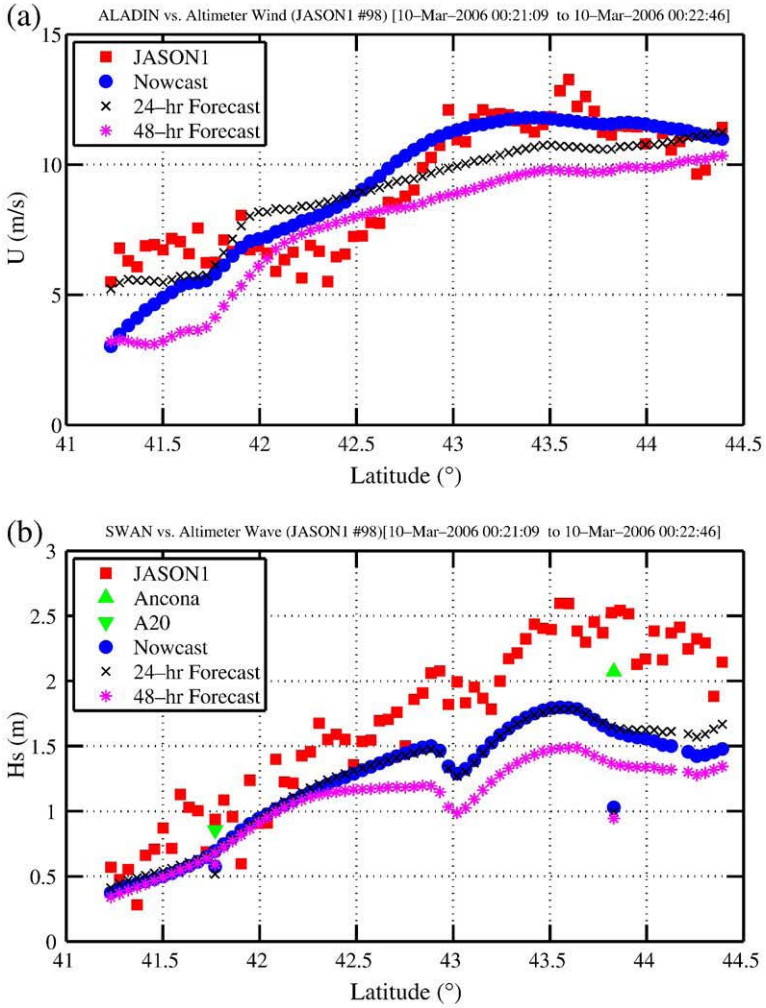

Fig. 11. Comparisons of JASON-1 altimeter wind and wave data along track No. 98 against interpolated (a) ALADIN U_{10} and (b) SWAN H_s of 0-h nowcast, 24-h, and 48-h forecasts. Also shown in (b) are in-situ H_s from A20 and Ancona buoy interpolated at 0 UTC, March 10, 2006 and their corresponding SWAN forecast H_s. The *x*-axis coordinate is expressed as the latitude coordinate of the altimeter footprints, A20 and Ancona buoy.

4.2. Comparisons with altimeter data

Model validation against in-situ measurements away from the coasts to cover the entire Adriatic Sea is logistically and financially impractical. In practice, model evaluations over a large area can be carried out by comparing against measurements from satellite altimeters (Hwang et al., 1999; Cavaleri and Sclavo 2006; Ardhuin et al., 2007). For the period from mid-September 2005 through mid-October 2006, altimeter U_{10} and H_s data were obtained from three satellites: (1) ENVISAT (European Space Agency), (2) JASON-1 (NASA/Centre Nationale d'Études Spatiales), and (3) GFO (the US Navy Geosat Follow-On). The altimeter footprints along the satellite tracks provide a large spatial coverage that cannot be accomplished by in-situ observation at a few fixed stations. The ground tracks over the Adriatic Sea during the DART project period are shown in Fig. 9. The combined coverage from tracks of the three satellites is extensive and relatively uniform over the Adriatic Sea. The details of those satellite observations and their accuracy which is considered good for most practical purposes can be found in Resti et al. (1999), Menard et al. (2003), and Durrant and Greenslade (2007). For their calibration techniques, Cavaleri and Sclavo (2006) compared ERS-1 altimeter H_s to buoy measurements in the Mediterranean, including those within the Adriatic, reporting minimal altimeter bias with accuracy of 2 m/s for winds and 10% for waves. Since then updated satellite-based measurements have improved.

The satellite-borne altimeters can fly over the Adriatic Sea in a very short time and provide a snapshot of the spatial variation of both wind and wave fields along its track. During a sirocco wind event in March 2006, the JASON-1 satellite crossed over the area within 97 s (0:21:09 to 00:22:46 UTC on March 10, 2006 along track No. 97) starting from the southern Italian coast northwestward across the Adriatic Sea to the northern Croatian coast providing altimeter measurements depicting wind and wave spatial variations. Comparisons of altimeter data and ALADIN and SWAN model results provide a validation of model performance in predicting spatial variation over a larger area. We compared altimeter data against model wind and wave field at 00 UTC, March 10, 2006 (Fig. 10), which is represented by the nowcast run at 00 UTC, March 10, 2006 and the 24-h and 48-h forecasts, respectively, run earlier at 00 UTC March 9 and 00 UTC March 8. The JASON track No. 98 is overlaid on the model wind and wave field shown as white dashed line. The nowcast results show that large winds and waves concentrated in areas just off the Croatian coast. These spatial variations are also shown in the 24-h and 48-h forecasts. The only noticeable difference among them is the intensity and size of high wind and wave areas. For comparison to the altimeter data, both SWAN wave and ALADIN wind results were spatially interpolated from model grid points to the position of altimeter footprints along the track. Fig. 11 shows the spatial variation of H_s along the track measured by the altimeter and predicted by the interpolated model results of the nowcast, 24-h and 48-h forecasts. Both model and altimeter results similarly show increasing U_{10} and H_s from south to north. The nowcast ALADIN U_{10} agree better with altimeter U_{10} than those from the 24-h and 48-h forecast. The altimeter H_s increases from less than 0.5 m to 2.5 m along the track. The nowcast H_s from SWAN was significantly underpredicted with heights only up to 1.7 m. Also, the underestimation is somewhat larger for both U_{10} and H_s in the 48-h forecast compared to the 24-h forecast and the nowcast. In addition, Fig. 11 includes the model and measured H_s for the Ancona buoy location. The difference in H_s between the Ancona buoy and the altimeter track are very similar to each other in both the model results and measurements indicating a good prediction of the sirocco H_s spatial pattern, but the absolute value of the underprediction by the model at Ancona could have posed operational difficulties in the use of this result.

To further extend the comparison beyond this single snapshot along this satellite track, wind and wave model results were spatially and temporally interpolated to collocate with altimeter data. To do this, hourly model U_{10} and H_s within 60 min of the altimeter collection time were spatially interpolated from the grid points to the locations of the altimeter measurements along the satellite tracks, which is very similar to the method used by Cavaleri and Sclavo (2006). We grouped model results of nowcast and hourly forecasts up to 11-h in order to assemble a larger number model output data points and thus increase statistical significance. Fig. 12 shows the scatter plot of altimeter versus model data. The correlation coefficients between these altimeter measurements and ALADIN wind and SWAN wave predictions are 0.78 and 0.79, respectively. Model wind speeds were slightly lower than altimeter wind speeds (about 4%) as indicated by the 0.96 value of the best-fit slope. The SWAN H_s was underpredicted by an average of 30% with a best-fit slope value of 0.7. The comparison of altimeter and forecast results for increasing forecast hour (not shown) showed a very similar underprediction with slightly increasing data scatter.

Based on the best-fit slope values as shown in Figs. 12 and 13, the bias of U_{10} produced by the 8-km operational high-resolution ALADIN against altimeter U_{10} was small bias about 4%, while SWAN H_s show a

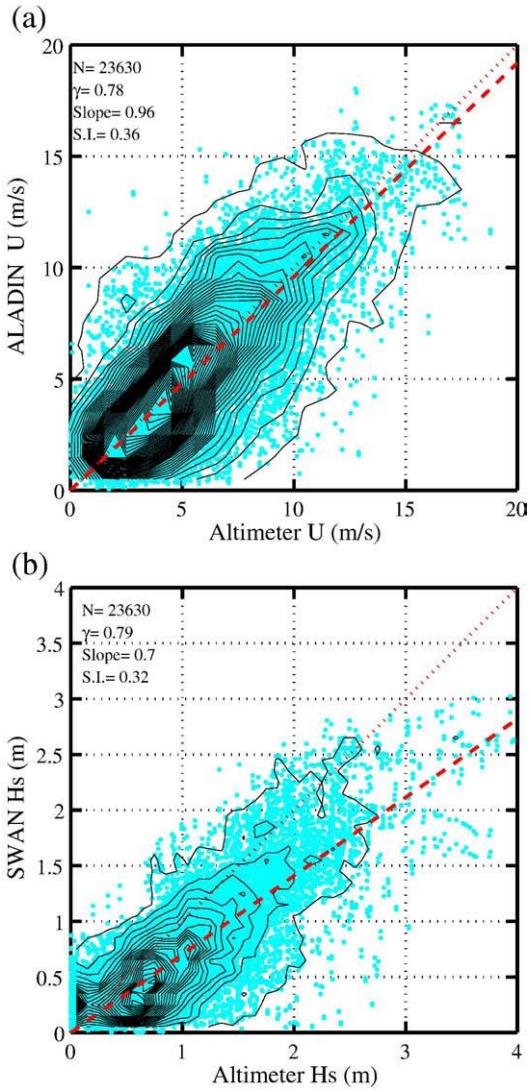

Fig. 12. Comparisons of altimeter observations to model hourly output from nowcast through 11-h forecast: (a) U_{10}: ALADIN against altimeter wind. (b) H_s: SWAN against altimeter wave. The dotted line shows the 1:1 agreement target. The dashed lines are the best-fit line. The contour lines indicate density of data number distribution with an interval of 20 starting at 5.

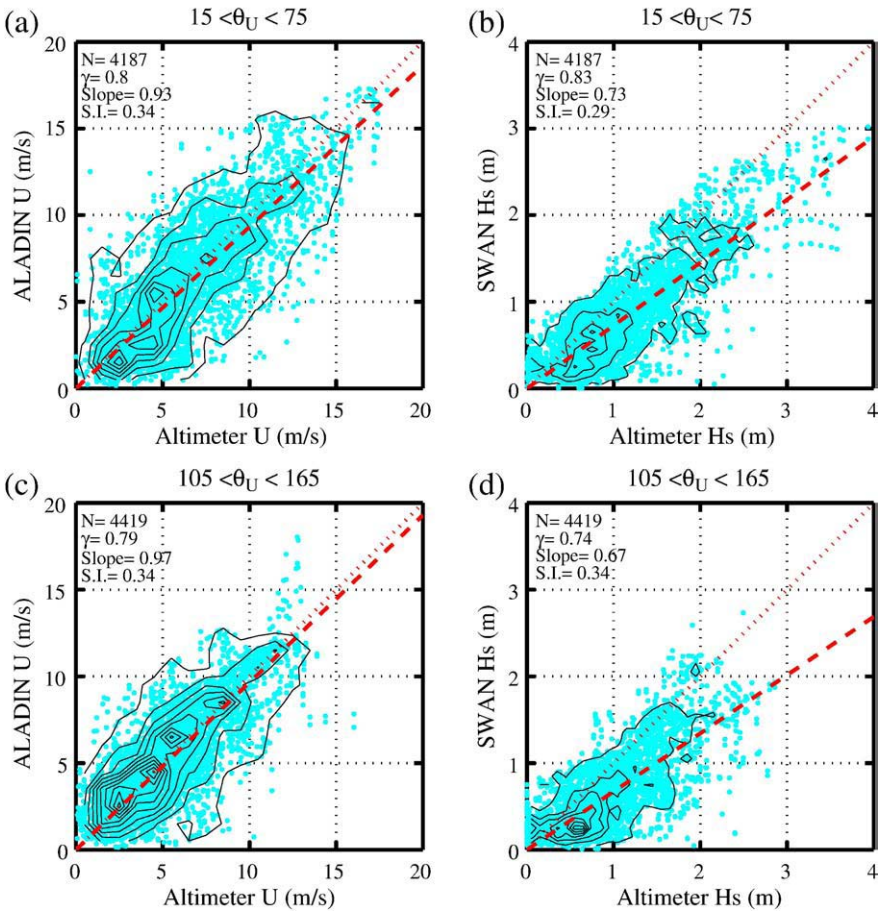

Fig. 13. Scatter plots of altimeter against model nowcast data for northeasterly wind fetch condition: (a) U_{10} and (b) H_s, and for southeasterly wind fetch condition: (c) U_{10} and (d) H_s. The dotted line shows the 1:1 agreement target. The dashed lines are the best-fit lines. The contour lines indicate density of data distribution with an interval of 20 starting at 5.

very significant underprediction (30%). To examine the possible error of H_s underestimation due to errors in the model U_{10}, we re-ran SWAN using slightly higher modeled U_{10} (multiplying ALADIN U_{10} by a factor of 1.1). The best-fit slope between the altimeter and SWAN H_s forced by the higher U_{10} increased to 0.83 (an underprediction by 17%). This represents an 18% change in H_s for a 10% increase in U_{10}. This change is consistent with the generalized wind–wave dependence relation, which indicates the rate of change in waves ΔH (%) is related to the rate of change in wind ΔU (%) by $\Delta H = \beta \Delta U$, where β is an empirical value varying between 1 for strong fetch-limited wave growth and 2 for fully-developed equilibrium condition (Cavaleri and Bertotti, 2006; Arduin et al., 2007). Nevertheless, this numerical exercise shows that the 30% SWAN wave underprediction cannot be explained and attributed to the 4% underprediction in input ALADIN winds.

To investigate the model performance under different wind–wave generation conditions, we studied model wind and wave performance under particular cross-basin (northeasterly) and along-basin (southeasterly) winds representing shorter fetch and longer fetch conditions, respectively. The northeasterly cross-basin wind is represented by data with ALADIN wind directions ranging from 15 and 75°. The southeasterly along-basin wind is represented by data with ALADIN wind directions ranging from 105 to 165°. The comparisons between altimeter and model results under these two different fetch conditions are shown in Fig. 13. While the ALADIN U_{10} of both fetch conditions remain very close to altimeter U_{10} with best-fit slopes of 0.93 and 0.96, respectively, for northeasterly and southeasterly winds (Fig 13a and c), the underestimation of SWAN H_s are 27% and 33%, respectively, for shorter (northeasterly) and longer (southeasterly) fetches. This implies that the SWAN underpredictions cannot be attributed to the difference in wind fetch conditions.

A complete investigation of ALADIN wind model accuracy is beyond the scope of this work, but we do note that in various dedicated studies the 8-km operational ALADIN model has been found to produce reasonable wind fields over the sea for most of the specific wind types (bora studied in Ivatek-Šahdan and Tudor, 2004; Janeković and Tudor, 2005; sirocco studied in Pasarić et al., 2007; etesian and sea–land breezes studied in Klaić et al., 2009-this issue) that impact the Adriatic Sea. This is in large part due to resolving the complicated orography surrounding the Adriatic which allows for the production of realistic small-scale structures and mountain effects in the winds. Based on these other studies it seems unlikely that there are overall errors in ALADIN wind patterns sufficient to cause the general SWAN wave underpredictions.

4.3. Geographical variability of model performance

We then further examine the spatial variability of wave model performance based on the method proposed by Cavaleri and Bertotti (2006). All space and time collocated model and altimeter data used in Fig. 12 are then regrouped into subsets of grid cells (1° in longitude and 1° in latitude) according to the coordinates of co-located model and altimeter data. Mean values of altimeter and model data and comparison results between model and altimeter data represented by the values of best-fit linear slope and scatter index were obtained at each cell. The statistical results are then presented at each cell's center coordinates (Figs. 14 and 15). For smooth and stable results, a 1° moving-cell mean was applied with a 0.1° interval on both longitude and latitude directions.

Two-dimensional contour plots of spatial distributions of the mean values of altimeter and model U_{10} and H_s during the DART project are

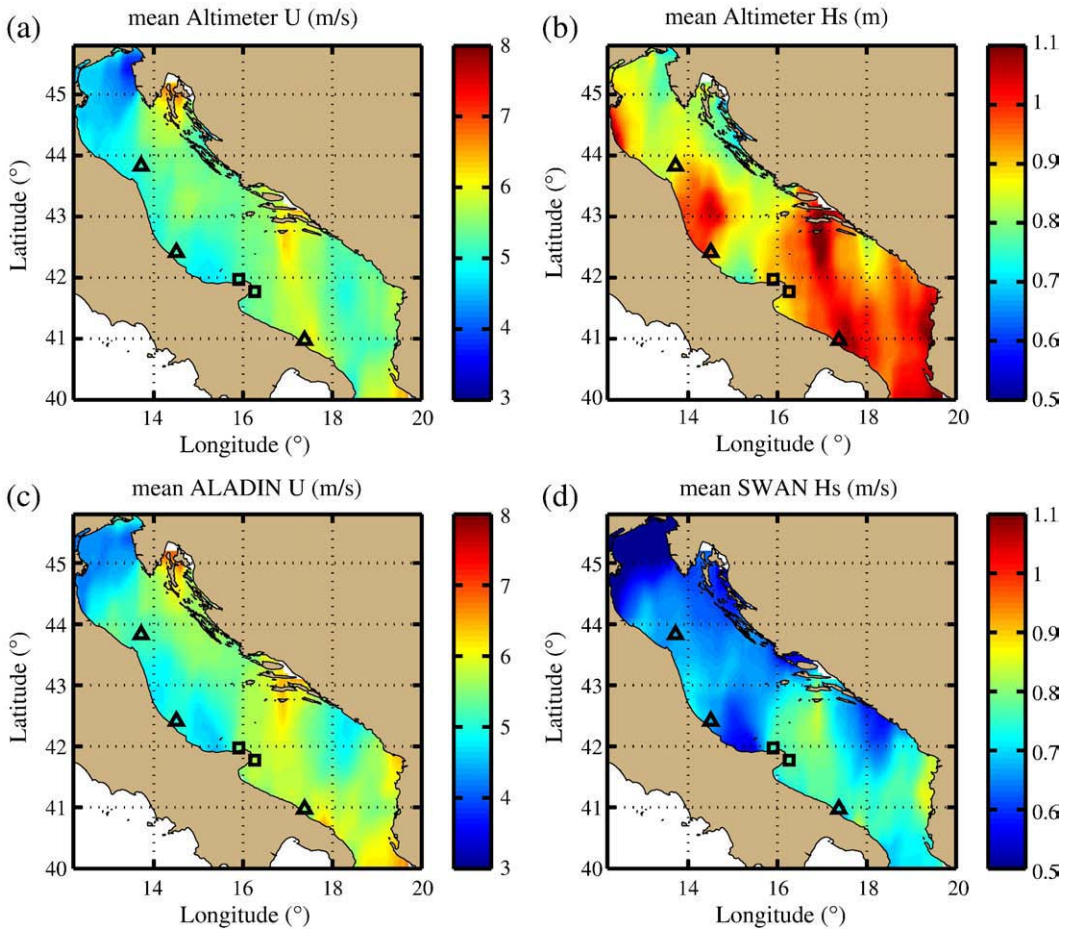

Fig. 14. Geographical distribution of cell-averaged wind and wave. (a) altimeter U_{10} , (b) altimeter H_s, (c) ALADIN U_{10} , and (d) SWAN H_s. Locations of in-situ measurements of DART ADCP Wave Array (squares) and RON buoys (triangles).

shown in Fig. 14. Most of mean U_{10} in this region vary between 5 and 6 m/s. In the areas near the northern corner of the Adriatic Sea, the mean U_{10} dropped to about 4 m/s. For two small areas off the Croatian coast, the mean U_{10} exceeded 6 m/s. Both the magnitude and spatial variability of mean ALADIN U_{10} (Fig. 14c) are very similar to those of altimeter U_{10} (Fig. 14a). The corresponding mean altimeter H_s (Fig. 14b) shows a variation from 0.7 to 1.1 m. In a few areas off the Italian coast mean H_s was larger than 1 m. The mean values of altimeter H_s in Croatian coastal waters around 42.7° N and 17° E are very large, and this corresponds well to the high wind area shown in Fig. 14a. However, the spatial distribution of mean SWAN H_s shows significantly smaller mean values everywhere and less spatial variation (Fig. 14d) with mean H_s varying only from 0.5 to 0.8 m.

The spatial distributions of best-fit slope, scatter index and correlation coefficient for comparison between altimeter and model data are shown in Fig. 15. In general, the distribution of best-fit slope for the U_{10} comparison is very uniform with slope values near unity. It shows that ALADIN U_{10} was generally within 10% of altimeter U_{10} over the Adriatic Sea. This variation pattern is consistent with the observed good agreement of mean U_{10} distributions of altimeter and ALADIN values shown in Fig. 14a and c. The spatial distribution of best-fit slope for wave comparisons, however, shows a much larger spatial variability with slope values varying from 0.5 to 0.8 indicating a significant location-dependent SWAN H_s underestimation of 20% to 50% (Fig. 15b). Larger H_s underpredictions are shown in waters off both the Italian and Croatian coasts. In the coastal waters just off Cape Gargano (42° N and 16° E), where GS1 and A20 are located (indicated by squares), the H_s underprediction is relatively small with best-fit slope values exceeding 0.8. These slope values are close to those of the in-situ, specific-location comparisons shown in Fig. 6. The best-fit slope values between altimeter and model waves near the Ortona buoy are around 0.7 or less, which is also consistent with those from the in-situ, specific-location comparison (Fig. 7d). The largest SWAN H_s underprediction (about 50%) is in the semi-enclosed coastal waters at the very northwestern corner of Adriatic Sea (area centering around 45.2° N and 13.5° E). In the area just southeast of the largest underperformed area (around 44.5° N and 13.2° E), SWAN H_s underprediction is much smaller with the best-fit slope up to 0.8. The region of larger H_s underprediction near the Strait of Otranto is likely related to the neglect of incoming wave energy at this open boundary. However, the limited spatial extent of this region suggests that the influence of such waves is confined to this region and does not extend far into the Southern Adriatic proper.

Scatter index values of H_s comparisons vary mostly around 0.3 except those in the area off the Croatian coast between 44° and 45° N, where the scatter index increases to 0.5. In general, the data scatter of the wind comparison is larger than those of wave comparison with their values varying around 0.4.

Spatial variability of wind and wave model performance in terms of slope values and scatter index has been shown in model evaluation studies by Cavaleri and Bertotti (2004, 2006) and Cavaleri and Sclavo (2006) for the Mediterranean Sea. For both wind and H_s the best-fit slope increases moving away from northern coast of the Mediterranean Sea based upon their comparisons of a lower-resolution wave model forced by lower-resolution winds against altimeter data. The values of the best-fit slope between model and altimeter H_s in the Adriatic Sea as shown in Fig. 11 of Cavaleri and Sclavo (2006) are in the range of 0.48 to 0.72. Using higher-resolution wind and wave models,

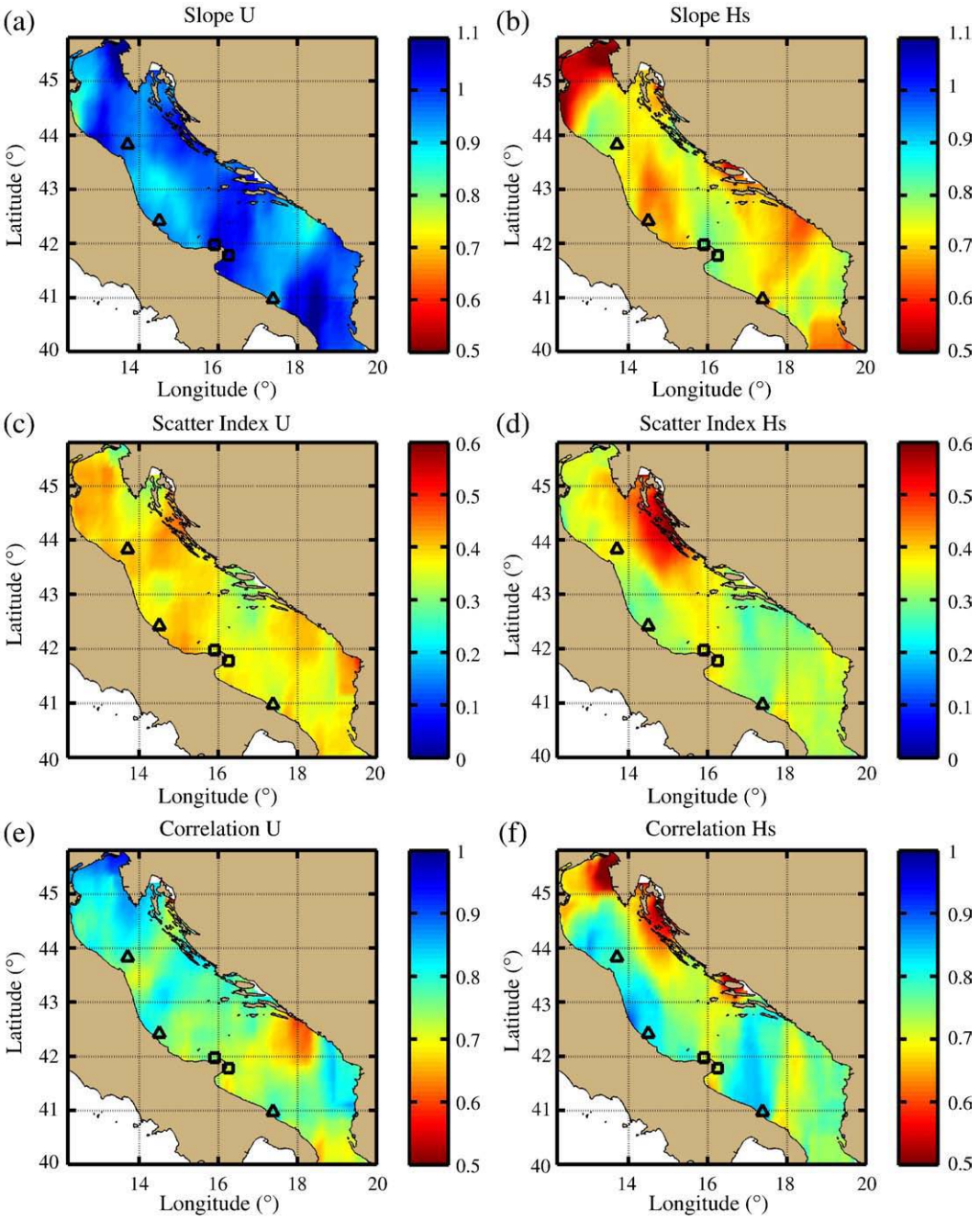

Fig. 15. Geographical distribution of cell-averaged best-fit slope, scatter index, and correlation coefficient for comparisons between altimeter and model results. Best-fit slope for (a) U_{10} and (b) H_s. Scatter index for (c) U_{10} and (d) H_s. Correlation coefficient for (e) U_{10} and (f) H_s. Locations of in-situ measurements of DART ADCP Wave Array (squares) and RON buoys (triangles).

our range, 0.5 to 0.8, is very similar, but the spatial patterns are different with the exception of the northwest corner where both our results and those of Cavaleri and Sclavo (2006) show H_s underestimation of nearly 50%. We find an even greater difference between the best-fit slope (bias corrections) for wind and H_s than Cavaleri and Sclavo (2006). They suggest that the error is more likely to be in the wind field rather than in the wave model. In contrast, with a different wind and wave model, we find that using a wind model with better resolution and better ability to represent the complex orography greatly improves the best-fit slope for the wind but not for the waves compared to their results.

Also our scatter index range, 0.22 to 0.5, is very similar to the Adriatic Sea scatter index range in Fig. 9 of Cavaleri and Sclavo (2006), 0.28 to 0.55. This is consistent with the findings of Signell et al. (2005) who found similar H_s correlation values between wave buoys and SWAN models forced by high- and low-resolution wind products. They partially attributed this to low-frequency space and time errors that are passed to the higher-resolution models from the lower-resolution models in which they are nested. Our patterns of higher scatter index distinctly differ from those of Cavaleri and Sclavo (2006). Their pattern in the Adriatic Sea shows a general southeast to northwest gradient of scatter index that they suggest is related the orography and the wind field, while our pattern shows a few localized regions of high scatter index and a broad region of high scatter index along and offshore of the central Croatian coast. Our scatter index results might also be related to wind accuracy but do not show indications of direct broad scale association with orography.

5. Discussion and concluding remarks

We have used five different wave buoys/moorings and three separate altimeter satellites to evaluate the performance of one high-resolution wave model forced by operationally high-resolution winds over the year of the DART experiment. This wind and wave models performed reasonably well from an operational standpoint, correctly predicting the timing and spatial variance of a bora that took place during March, one of the months with maximum mooring work requirements. Though the wave model forecast of H_s during a sirocco preceding the bora was significantly underestimated, the spatial variability of the overall forecast could have provided useful guidance for making operational decisions. Overall, the 24-h forecast of wave events was highly correlated (0.82–0.91) with the measured time-series of H_s at the buoy locations. However, it is also clear that a few wave events at other times were not predicted so well, and that overall there was a time averaged spatial-median underprediction of H_s with significant spatial variance.

Unlike the previous studies that could attribute underprediction of H_s to unresolved scales and bias in the wind field, the ALADIN wind field used in this study shows a relatively low bias (4%) and the wind speeds would have to be enhanced to many times this bias in order to remove the observed SWAN H_s bias. Systematic errors have not been found in limited studies of various types of ALADIN wind events and the spatial pattern of H_s bias does not seem to follow a known wave pattern of a particular Adriatic wind event. Rather the underprediction of H_s everywhere with such low bias wind forcing and the independence of this result on short or long fetches suggests that there may be a more fundamental issue with the wave model dynamics or wind–wave coupling that needs further investigation.

With some local exceptions, the spatial pattern of the scatter index for H_s does not match the spatial pattern of the scatter index of the wind speed, i.e. regions of relative accuracy/inaccuracy of the winds and H_s did not coincide. In the Croatian portion of the Adriatic between 43° N and 45° N the scatter index for the H_s comparisons for a broad region indicated a particularly high error. This region generally has higher H_s for sirocco storms, slightly suggesting that SWAN might have greater difficulty with such wind types in this particular region. This map could be used to guide further investigation of SWAN performance and focus efforts for model improvement, but also this type of knowledge and such maps can serve as a tool to assist operational users in attaching the appropriate situation-dependent confidence in the SWAN output.

There is a need for further work regarding operational wave model evaluation. For example, differences between a model wave prediction of 3 m H_s and a measured H_s of 5 m might significantly contribute to overall model bias or scatter index but both these values may be above operational thresholds for ship activity and therefore such a difference might be unimportant for support of REA. In this way, standard model performance metrics do not stand alone as the best evaluation tool for operational models. In this paper, we combine standard metrics with operational event orientated ones to provide a more complete picture of model performance.

Acknowledgements

Thanks to the captains, crews, and scientists of R/V G. Dallaporta, R/V Alliance, and R/V Universitatis. The success of the field work was in large part due to the dedicated efforts of Mark Hulbert, Andrew Quaid, and Wesley Goode of the NRL technical team. Michel Rixen of the NATO Undersea Research Centre (NURC) led and organized the larger international DART collaborative project and contributed in many ways to this work. The NRL DART project greatly benefited from being part of a NURC/NRL Joint Research Project and from contributions from many international partners. ALADIN products were from the Croatian Meteorological and Hydrological Service and were provided through the work of Martina Tudor. We thank APAT for sharing RON wave buoy data. We thank Jacopo Chiggiato and Servizio Idro-Meteo-Clima ARPA-SIMC of Emilia Romagna Region, Bologna, Italy for allowing us to use a snapshot of their SWAN model in the paper; we thank Anneta Mantziafou and the University of Athens for allowing us to use a snapshot of their WAM model in the paper; and we thank Luigi Cavaleri and the Marine Science Institute of the Italian National Research Council for allowing us to use a snapshot of their WAM model in the paper. The research in this paper was supported by the Office of Naval Research as part of the "Dynamics of the Adriatic in Real-Time" and research programs under Program Element Number 0602435 N. This is NRL contribution NRL JA/7320-2008-8156. Finally, we thank the reviewers for their thoughtful and constructive comments to help improve this manuscript.

References

Allard, R.A., Kaihatu, J., Hsu, Y.L., Dykes, J.D., 2002. The integrated ocean prediction system. Oceanography 15, 67–76.
Allard, R.A., Dykes, J.D., Hsu, Y.L., Kaihatu, J.M., Conley, D., 2007. A real-time nearshore wave and current prediction system. J. Mar. Syst. 69, 37–58.
Ardhuin, F., Bertotti, L., Bidlot, J.-R., Cavaleri, L., Filipetto, V., Lefevre, J.-M., Wittmann, P., 2007. Comparison of wind and wave measurements and models in the Western Mediterranean Sea. Ocean Eng. 34, 526–541.
Arena, G., Briganti, R., Corsini, S., Franco, L., 2001. The Italian wave measurement buoy network: 12 years management experience. Proc. 4th Int. Symp. on Wave Measurement and Analysis, pp. 86–94.
Bertotti, L., Cavaleri, L., Tescaro, N., 1996. Long term wave hindcast in the Adriatic Sea. Il Nuovo Cimento C, vol 19, No. 1, pp. 91–108.
Bolanos-Sanchez, R., Sanchez-Arcilla, A., Cateura, J., 2007. Evaluation of two atmospheric models for wind–wave modelling in the NW Mediterranean. J. Mar. Syst. 65, 336–353.
Booij, N., Ris, R.C., Holthuijsen, L.H., 1999. A third-generation wave model for coastal region: 1. Model description and validation. J. Geophys. Res. 104 (C4), 7649–7666.
Cavaleri, L., 2002. Final report of the European Centre for Medium-range Weather Forecasts special project: Testing and application of a third generation model in the Mediterranean Sea. WWW Page, http://www.ecmwf.int/about/special_projects/finished_projects/cavaleri_med-sea-wam3/report_2002.pdf.
Cavaleri, L., Bertotti, L., Lionello, P., 1989. Wind waves evaluation in the Adriatic and Mediterranean Seas. Int. J. Numer. Methods Eng. 27, 57–69.
Cavaleri, L., Bertotti, L., Tescaro, N., 1996. Long term wind hindcast in the Adriatic Sea. Il Nuovo Cimento C, Vol 19, No. 1, pp. 67–89.
Cavaleri, L., Bertotti, L., 1997. In search of the correct wind and wave fields in a minor basin. Mon. Wea. Rev. 125 (8), 1964–1975.
Cavaleri, L., Bertotti, L., 2004. Accuracy of the modelled wind and wave fields in enclosed seas. Tellus 56A, 167–175.
Cavaleri, L., Bertotti, L., 2006. The improvement of modeled wind and wave fields with increasing resolution. Ocean Eng. 33, 553–565.
Cavaleri, L., Sclavo, M., 2006. The calibration of wind and wave model data in the Mediterranean Sea. Coastal Eng. 53, 613–627.
Cushman-Roisin, B., Gačić, M., Poulain, P.-M., Artegiani, A. (Eds.), 2001. Physical Oceanography of the Adriatic Sea: Past, Present and Future. Kluwer Academic Publishers, Dordrecht.
Durrant, T.H., Greenslade, D.J.M., 2007. Validation and application of Jason-1 and Envisat significant wave heights. Proc. 10th Int. Workshop on Wave Hindcasting and Forecasting and Coastal Hazards Symp., Hawaii, USA.
Dykes, J.D., Allard, R.A., Blain, C.A., Estrade, B., Keen, T.R., Smedstad, L.F., Walcraft, A.J., 2004. An approach for coupling diverse geophysical and dynamical models. NRL Rev. 167–169.
Holthuijsen, L.H., Booij, N., Herbers, T.H.C., 1989. A prediction model for stationary, short-crested waves in shallow water with ambient currents. Coast. Eng. 13, 23–54.
Hsu, Y.L., Rogers, W.E., Dykes, J.D., 2002. WAM performance in the Gulf of Mexico with COAMPS wind. Proc. 7th Int. Workshop on Wave Hindcasting and Forecasting. Banff, Alberta, Canada, pp. 151–159.
Hwang, P., Bratos, S.M., Teague, W.J., Wang, D.W., Jacobs, G.A., Resio, D.T., 1999. Winds and waves in the Yellow and East China Seas: spaceborne altimeter measurements and model results. J. Phys. Oceanogr. 55, 307–325.
Ivatek-Šahdan, S., Tudor, M., 2004. Use of high-resolution dynamical adaptation in operational suite and research impact studies. Meteorologische Zeitschrift, 13 (2), 99–108 (10).
Janeković, I., Tudor, M., 2005. The Adriatic Sea wave response to severe bura wind. Proc.28th Int. Conf. on Alpine Meteorology (ICAM) and Annual Scientific Meeting of the Mesoscale Alpine Programme. WWW page, http://www.map.meteoswiss.ch/map-doc/icam2005/proceedings.html.
Janssen, P.A.E.M., Hansen, B., Bidlot, J.R., 1997. Verification of the ECMWF wave forecasting system against buoy and altimeter data. Weather Forecast 12, 763–784.
Jensen, R.E., Wittmann, P.A., Dykes, J.D., 2002. Global and regional wave modeling activities. Oceanography 15, 57–66.
Kallos, G., Kotroni, V., Lagouvardos, K., 1997. The regional weather forecasting system SKIRON: an overview. Proc. Symp. Regional Weather Prediction on Parallel Computer Environments. University of Athens, Greece, pp. 109–122.
Kallos, G., Papadopoulos, A., Katsafados, P., Nickovic, S., 2006. Transatlantic Saharan dust transport: model simulation and results. J. Geophys. Res. 111, D09204.

Klaić, Z., Pasarić, Z., Tudor, M., 2009. On the interplay between sea–land breezes and etesian winds over the Adriatic, J. Mar Syst., this issue.
Komen, G.J., Cavaleri, L., Donelan, M., Hasselmann, K., Hasselmann, S., Janssen, P.A.E.M., 1994. Dynamics and Modelling of Ocean Waves. Cambridge University Press, New York.
Lenartz, F., Beckers, J.-M., Christiaen, B., Champenois, W., Troupin, C., Vandenbulke, L., Rixen, M., 2007. Wave forecast with a super-ensemble. Rapid Environment Assessment Conf., Lerici, Italy.
Ménard, Y., Fu, L., Escudier, P., Parisot, F., Perbos, J., Vincent, P., Desai, S., Haines, B., Kunstmann, G., 2003. The Jason-1 mission. Mar. Geodesy 26, 131–146.
Pasarić, Z., Belušić, D., Klaić, Z.B., 2007. Orographic influences on the Adriatic sirocco wind. Ann. Geophys. 25, 1263–1267.
Pasarić, Z., Belušić, D., Chiggiato, J., 2009. Orographic effects on meteorological fields over the Adriatic from different models. J. Mar. Syst., this issue.
Piscopia, R., Inghilesi, R., Panizzo, A., Corsini, S., Franco, L., 2002. Analysis of 12-year wave measurements wave measurements by the Italian wave network. Proc. Coast. Eng. Conf., pp. 121–133.
RD Instruments, 2001. Waves User's Guide. P/N 957-6148-00 (April 2001), Teledyne RD Instruments, 14020 Stowe Dr., Poway, CA, 92064.
Resti, A., Benveniste, J., Roca, M., Levrini, G., Johannessen, J., 1999. The Envisat radar altimeter system (RA-2). ESA Bulletin 98, 94–101.
Ris, R.C., Booij, N., Holthuijsen, L.H., 1999. A third-generation wave model for coastal regions: part II—verification. J. Geophys. Res. 104 (C4), 7667–7681.
Rogers, W.E., Kaihatu, J.M., Petit, H.A.H., Booij, N., Holthuijsen, L.H., 2002. Diffusion reduction in an arbitrary scale third generation wind wave model. Ocean Eng. 29 (11), 1357–1390.
Rogers, W.E., Hwang, P.A., Wang, D.W., 2003. Investigation of wave growth and decay in the SWAN model: three regional-scale applications. J. Phys. Oceanogr. 33, 366–389.
Rogers, W.E., Kaihatu, J.M., Hsu, Y.L., Jensen, R., Dykes, J.D., Holland, T., 2007. Forecasting and hindcasting with the SWAN model in the Southern California Bight. Coastal Eng. 54 (1), 1–15.
Signell, R.P.S., Carniel, S., Cavaleri, L., Chiggiato, J., Doyle, J.D., Pullen, J., Scavo, M., 2005. Assessment of wind quality for oceanographic modelling in semi-closed basins. J. Mar. Syst. 53, 217–233.
Steppeler, J., Doms, G., Schättler, U., Bitzer, H.W., Gassmann, A., Damrath, U., Gregoric, G., 2003. Meso-gamma scale forecasts using nonhydrostatic model LM. Meteorol. and Atmos. Phys. 82, 75–96.
Strong, B., Brumley, B., Terray, E.A., Stone, G.W., 2000. The performance of ADCP-derived directional wave spectra and comparison with other independent measurements. Proc. MTS/IEEE Oceans 2000 Conf. Rhode Island, USA, Providence, pp. 1195–1203.
WAMDI Group, 1988. The WAM model — a third-generation ocean wave prediction model. J. Phys. Oceanogr. 18, 1775–1810.